Supporting Information

Performance Analysis of Perovskite Solar Cells using DFT Extracted Parameters of Metal-Doped TiO_2 Electron Transport Layer

Sadiq Shahriyar Nishat[‡§], Md. Jayed Hossain[±§], Faiyaz Elahi Mullick[±], Alamgir Kabir[‡], Shaestagir Chowdhury[ǂ], Sharnali Islam[±], and Mainul Hossain[±]*

[‡]Department of Physics, University of Dhaka, Dhaka-1000, Bangladesh
[±]Department of Electrical and Electronic Engineering, University of Dhaka, Dhaka-1000, Bangladesh
[ǂ]Department of Mechanical and Materials Engineering, Portland State University, Portland, OR 97201, United States

*Corresponding author e-mail: mainul.eee@du.ac.bd

[§]Equal contribution

S1. Macroscopic Charge Carrier Mobility Calculations in TiO_2 using DFT:

The semiclassical Boltzmann theory, within the constant relaxation time approximation (CRTA), has been used to determine the charge carrier mobility of pristine rutile TiO_2 and TiO_2 doped with Sn and Zn. To calculate the transport properties, the BoltzTrap2 code[1] is interfaced with VASP to read the non-self-consistent band information of the uniformly distributed *k*-mesh generated by VASP.[2,3]

For obtaining highly accurate results, we used 50 times more points in the real space than the number of *k*-points used in the reciprocal space for BoltzTrap2 calculations. In solving the Boltzmann equation, the energy range of the interpolation is limited to only within the VBM and the CBM edges. From the results, the carrier concentration-dependent effective mass of the carriers, at room temperature (300K), is calculated. The following graphs, in Figure S1 (a)-(h),

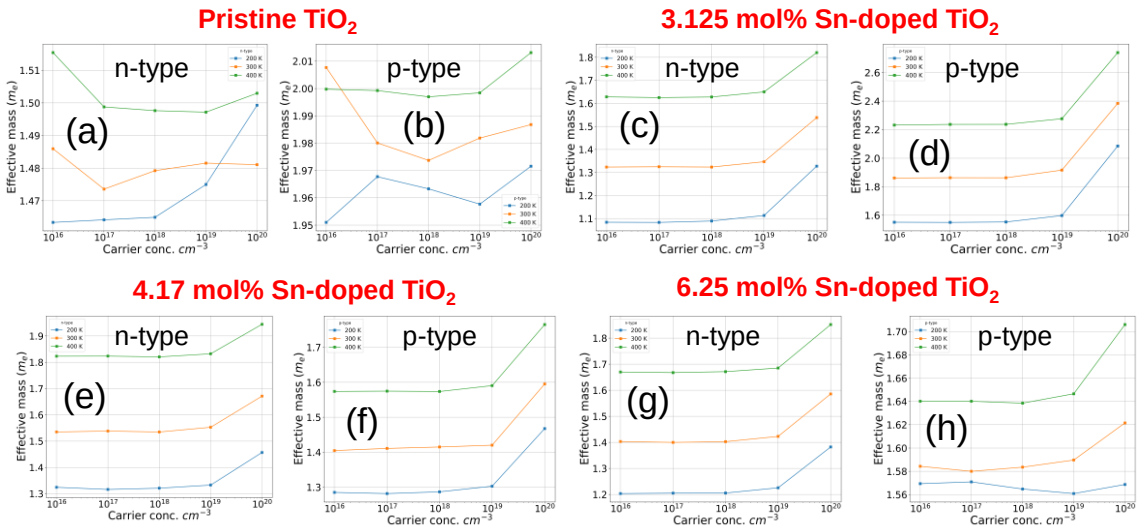

Figure S1. (a)-(h) Carrier concentration dependent effective mass for electrons (n-type) and holes (p-type) in pristine and Sn-doped TiO_2 at different temperatures (200 K, 300 K and 400 K).

show how the effective mass of electrons (n-type) and holes (p-type), vary with the carrier concentration at different temperatures (200 K, 300 K and 400 K), for pristine and Sn-doped TiO_2.

The effective mass of the carriers that correspond to the carrier concentration at room temperature (300 K) is first selected. The CRTA method then uses the following equation to calculate the mobility (μ), using the effective mass (m^*):

$$\mu = \frac{e\tau}{m^*} \tag{1}$$

where, e is the electronic charge and τ is the relaxation time. Finally, the carrier mobilities, calculated from the effective mass, are used as input parameters in the SCAPS-1D simulations to derive the electrical characteristics of the solar cell. Previous studies have used the well-established CRTA method for a wide range of thermoelectric materials.[4–6]

The relaxation time depends on different scattering phenomena including phonon, electron-phonon coupling, temperature, deformation potential, etc. However, in our work, we kept the relaxation time fixed (10^{-10}s)[7,8] for all calculations, such that the calculated electron mobilities of pristine and doped TiO_2 are of the same order of magnitude as those reported by Cai *et al.*[9]

Moreover, the DFT computed mobility values, along with the optical absorption spectrum, yield similar trends in PCE with changes in Sn doping concentration, as reported in the experimental studies by Cai *et al.*[9] and Liao *et al.*[10] Similar approach has been adopted by other groups to calculate mobilties.[11,12] Table S1 shows the carrier mobilities of pristine, Sn-doped and Zn-doped TiO_2, obtained using the CRTA method.

Table S1. Carrier mobilities of undoped and doped TiO_2 calculated with the constant relaxation time approximation (CRTA) method

TiO_2 layer	Electron mobility (cm^2/Vs)	Hole mobility (cm^2/Vs)
Pristine TiO_2	11.54×10^{-4}	8.90×10^{-4}
3.125 mol % Sn doped TiO_2	13.03×10^{-4}	9.16×10^{-4}
4.17 mol % Sn doped TiO_2	11.33×10^{-4}	12.30×10^{-4}
6.25 mol % Sn doped TiO_2	12.43×10^{-4}	11.06×10^{-4}
4.17 mol % Zn doped TiO_2	11.72×10^{-4}	8.71×10^{-4}

S2. Calculation of Optical properties of TiO_2 using DFT:

The optical properties of pure TiO_2 and Sn-doped TiO_2 are obtained from the DFT+*U* calculations. The optical properties are calculated by the dielectric function given by, $\varepsilon(\omega) = \varepsilon_1(\omega) + i\varepsilon_2(\omega)$. By integrating the matrix elements between unoccupied and occupied electronic states, the imaginary part of the dielectric function $\varepsilon_2(\omega)$ is calculated first using the following equation:

$$\varepsilon_2(\omega) = \frac{2e^2\pi}{\Omega\varepsilon_o}\sum_{k,v,c}\left|\left\langle\psi_k^c\left|u.r\right|\psi_k^v\right\rangle\right|^2\delta(E_k^c - E_k^v - E) \qquad (2)$$

where u is the vector that determines the polarization of the incident electric field, ω is the frequency of light, ψ_k^c and ψ_k^v are the conduction and valance band wave functions, respectively, at k. Since the real and the imaginary parts are connected by the transformation of Kramers-Kronig,

using this transformation the real part of the dielectric function, $\varepsilon_1(\omega)$ is calculated from the imaginary part, $\varepsilon_2(\omega)$. The absorption coefficient *α(ω)* and reflectivity *R(ω),* are calculated from the real and imaginary parts of the dielectric constant, using the following set of equations:[13,14]

$$\alpha(\omega) = \sqrt{2}\omega\left[\sqrt{(\varepsilon_1^2 + \varepsilon_2^2)} - \varepsilon_1\right]^{\frac{1}{2}} \quad (3)$$

$$R(\omega) = \left[\frac{\sqrt{(\varepsilon_1 + \varepsilon_2)} - 1}{\sqrt{(\varepsilon_1 + \varepsilon_2)} - 1}\right]^2 \quad (4)$$

To ensure that there is good convergence, different *k*-points mesh density have been used to test the convergence of the absorption spectrum. Results show that, 7×7×11, 4×4×3, 4×4×4, and 4×4×5 *k*-points density give well converged optical spectra for pure TiO_2, 3.125, 4.17 and 6.25 mol% Sn-doped TiO_2, respectively. For instance, Figure S2 below shows the excellent *k*-point convergence in the absorption spectrum for 4.17 mol% Sn-doped TiO_2.

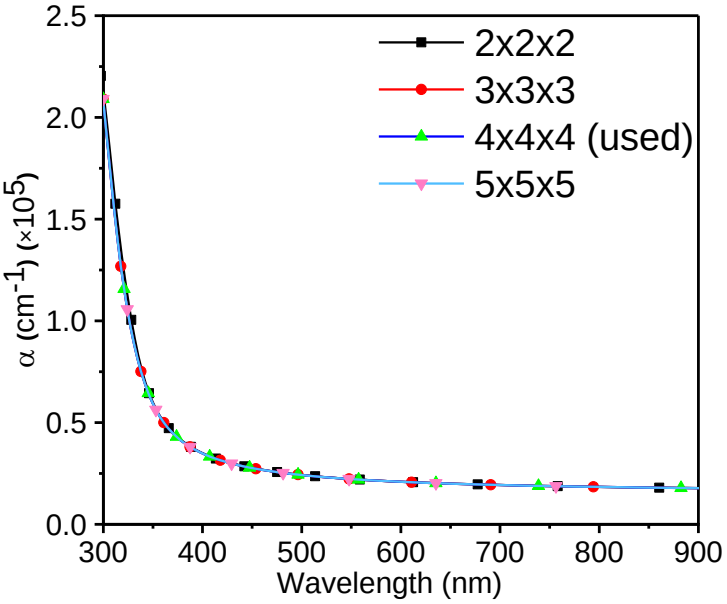

Figure S2. *k*-point convergence for 4.17 mol% Sn-doped TiO_2.

Table S2. Perovskite solar cell output characteristics obtained from SCAPS-1D using DFT extracted parameters of undoped and doped TiO_2

Electron Transport Layer	J_{SC} (mA/cm^2)	V_{OC} (V)	FF	PCE (%)
Pristine TiO_2	19.50	1.06	0.66	13.70
3.125 mol % Sn doped TiO_2	21.11	1.12	0.73	17.14
4.17 mol % Sn doped TiO_2	21.02	1.12	0.73	17.07
6.25 mol % Sn doped TiO_2	20.30	1.08	0.70	15.42
4.17 mol % Zn doped TiO_2	20.15	1.12	0.73	16.44

REFERENCES:

(1) Madsen, G. K. H.; Carrete, J.; Verstraete, M. J. BoltzTraP2, a Program for Interpolating Band Structures and Calculating Semi-Classical Transport Coefficients. *Comput. Phys. Commun.* **2018**, *231*, 140–145.

(2) Kresse, G.; Hafner, J. Ab Initio Molecular Dynamics for Liquid Metals. *Phys. Rev. B* **1993**, *47*, 558–561.

(3) Paier, J.; Hirschl, R.; Marsman, M.; Kresse, G. The Perdew-Burke-Ernzerhof Exchange-Correlation Functional Applied to the G2-1 Test Set Using a Plane-Wave Basis Set. *J. Chem. Phys.* **2005**, *122*, 234102.

(4) El-Mellouhi, F.; Madjet, M. E.; Berdiyorov, G. R.; Bentria, E. T.; Rashkeev, S. N.; Kais, S.; Akande, A.; Motta, C.; Sanvito, S.; Alharbi, F. H. Enhancing the Electronic Dimensionality of Hybrid Organic-Inorganic Frameworks by Hydrogen Bonded Molecular Cations. *Mater. Horizons* **2019**, *6*, 1187–1196.

(5) Zou, D.; Xie, S.; Liu, Y.; Lin, J.; Li, J. Electronic Structures and Thermoelectric Properties of Layered BiCuOCh Oxychalcogenides (Ch = S, Se and Te): First-Principles Calculations. *J. Mater. Chem. A* **2013**, *1*, 8888–8896.

(6) Lee, M. S.; Poudeu, F. P.; Mahanti, S. D. Electronic Structure and Thermoelectric Properties of Sb-Based Semiconducting Half-Heusler Compounds. *Phys. Rev. B - Condens. Matter Mater. Phys.* **2011**, *83*, 085204.

(7) Ozawa, K.; Emori, M.; Yamamoto, S.; Yukawa, R.; Yamamoto, S.; Hobara, R.; Fujikawa, K.; Sakama, H.; Matsuda, I. Electron-Hole Recombination Time at TiO_2 Single-Crystal Surfaces: Influence of Surface Band Bending. *J. Phys. Chem. Lett.* **2014**, *5*, 1953–1957.

(8) Yamada, Y.; Kanemitsu, Y. Determination of Electron and Hole Lifetimes of Rutile and Anatase TiO_2 Single Crystals. *Appl. Phys. Lett.* **2012**, *101*, 133907.

(9) Cai, Q.; Zhang, Y.; Liang, C.; Li, P.; Gu, H.; Liu, X.; Wang, J.; Shentu, Z.; Fan, J.; Shao, G. Enhancing Efficiency of Planar Structure Perovskite Solar Cells Using Sn-Doped TiO_2 as Electron Transport Layer at Low Temperature. *Electrochim. Acta* **2018**, *261*, 227–235.

(10) Liao, Y. H.; Chang, Y. H.; Lin, T. H.; Chan, S. H.; Lee, K. M.; Hsu, K. H.; Hsu, J. F.; Wu, M. C. Boosting the Power Conversion Efficiency of Perovskite Solar Cells Based on Sn Doped TiO_2 Electron Extraction Layer via Modification the TiO_2 Phase Junction. *Sol. Energy* **2020**, *205*, 390–398.

(11) Faghaninia, A.; Yu, G.; Aydemir, U.; Wood, M.; Chen, W.; Rignanese, G. M.; Snyder, G. J.; Hautier, G.; Jain, A. A Computational Assessment of the Electronic, Thermoelectric, and Defect Properties of Bournonite ($CuPbSbS_3$) and Related Substitutions. *Phys. Chem. Chem. Phys.* **2017**, *19*, 6743–6756.

(12) Motta, C.; El-Mellouhi, F.; Sanvito, S. Charge Carrier Mobility in Hybrid Halide Perovskites. *Sci. Rep.* **2015**, *5*, 12746.

(13) Gao, N.; Chen, W.; Zhang, R.; Zhang, J.; Wu, Z.; Mao, W.; Yang, J.; Li, X.; Huang, W. First Principles Investigation on the Electronic, Magnetic and Optical Properties of $Bi_{0.8}M_{0.2}Fe_{0.9}Co_{0.1}O_3$ (M = La, Gd, Er, Lu). *Comput. Theor. Chem.* **2016**, *1084*, 36–42.

(14) Abdul Rahim, N. A.; Ahmed, R.; Ul Haq, B.; Mohamad, M.; Shaari, A.; Ali, N.; Goumri-Said, S. Computational Modeling and Characterization of X-Bi (X = B, Al, Ga, In) Compounds: Prospective Optoelectronic Materials for Infrared/Near Infra Applications. *Comput. Mater. Sci.* **2016**, *114*, 40–46.